A Benchmark Slope For System Reliability Analysis

Jinsong Huang[1], M. ASCE, D.V. Griffiths[1,2], F. ASCE, Gordon A. Fenton[3] M. ASCE

[1]Centre for Geotechnical and Materials Modelling, Civil, Surveying and Environmental Engineering, The University of Newcastle, Callaghan, NSW 2308, Australia, Jinsong.huang@newcastle.edu.au
[2]Division of Engineering,Colorado School of Mines ,Golden, CO 80401,U.S.A, vgriffit@mines.edu
[3]Department of Engineering Mathematics, Dalhousie University, P.O. Box 1000, Halifax, Nova Scotia, Canada B3J 2X4, Gordon.Fenton@dal.ca

ABSTRACT: In a probabilistic slope stability analysis, the failure probability associated with the most critical slip surface (the one with the minimum reliability index) is known to be smaller than that obtained for the system as a whole where all potential slip surfaces are considered. System slope reliability has been studied in recent years by several probabilistic methods, including the Random Finite Element Method (RFEM), Limit Equilibrium Methods (LEM) combined with First Order Reliability Methods (FORM), and Response Surface Methods (RSM). The only one of these methods that can properly account for spatial variability however is the RFEM. In this paper, we set up a benchmark slope for system reliability analysis and compare the probability of failure obtained both with and without inclusion of spatial variability. The paper will give recommendations for the types of slope reliability problems that benefit from proper consideration of spatial variability.

INTRODUCTION

There are many potential slip surfaces in a slope, each of which has a finite probability of failure associated with it, so probabilistic slope stability analysis should be treated as a system reliability problem. As pointed out by Cornell (1967), a system's reliability is that of all potential slip surfaces, and the failure probability of a system will be larger than that for any single slip surface. The difference depends on the correlation between the failure probabilities of the different slip surfaces, for which no general formulation is available. System slope reliability has attracted a lot of research interests in recent years. Oka and Wu (1990) and Chowdhury and Xu (1995) presented system reliability analysis for a particular slope in which several slip surfaces were poorly correlated. Ching et al. (2009) analyzed several slopes using Monte Carlo simulation (MCS) and importance sampling (IS) methods. The results were compared with single-mode FORM analysis. It was then concluded that single-mode FORM analysis significantly underestimated the failure probability, and that

both the IS and MCS methods provided unbiased estimates of the failure probability. Huang et al. (2010) showed that the Random Finite Element Method (RFEM) can accurately predict the system probability of failure of slopes. Low et al. (2011) used multi-mode FORM to study reliability bounds of slopes.

In this paper, the slope studied by Ching et al. (2009) and Low et al. (2011) is chosen as a benchmark. Three types of analyses were conducted on this slope: (i) deterministic analyses were conducted to investigate failure regions, (ii) probabilistic analyses using Monte Carlo simulations were conducted to investigate the probability density function of the factor of safety (FS), and (iii) analyses were conducted to investigate the influence of spatial variability on the probability of failure (p_f).

DETERMINISTIC ANALYSIS

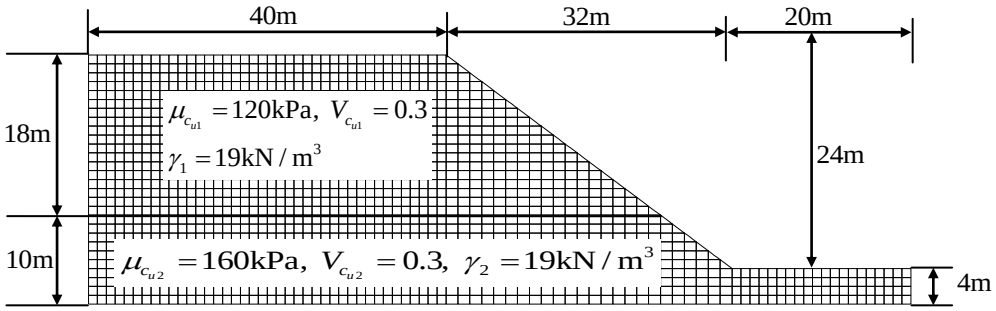

Fig. 1 A two layer undrained slope

The profile of the two layer undrained slope to be investigated is shown in Fig. 1. The slope has height $H = 24.0$ m . The upper layer has soil unit weight $\gamma_1 = 19.0$ kN/m^3 and shear strength $c_{u1} = 120.0$ kPa . The lower layer has the same unit weight but a different shear strength given by $c_{u2} = 160.0$kPa . Using the strength reduction method described by Griffiths and Lane (1999), the FS of the two layer slope was found to be 1.97. The deformed mesh at failure is shown in Fig. 2. It can be seen from Fig. 2 that the critical failure mode associated with the minimum FS goes deep and is almost circular.

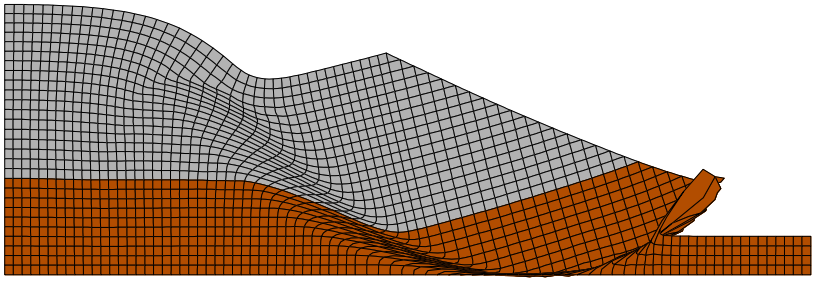

Fig. 2 Deformed mesh at failure when $c_{u1} = 120.0$ kPa, $c_{u2} = 160.0$kPa, $FS = 1.97$

In order to investigate failure regions, an exhaustive deterministic analysis was conducted by varying the strength of the two layers. The contours of FS are shown in Fig. 3. From the contour line of $FS = 1.0$, it is clear that there are three failure regions ($FS < 1.0$). The first one corresponds to a shallow failure mechanism which is caused by low strength of the upper layer (i.e., $c_{u1} < 50.0$ kPa). In this region, no matter how strong the lower layer is, the slope fails ($FS < 1.0$). The second failure region is associated with a deep failure mechanism which is caused by low strength of the lower layer (i.e., $c_{u2} < 40.0$ kPa). In this region, no matter how strong the upper layer is, the slope fails ($FS < 1.0$).The third failure region is the combination of c_{u1} and c_{u2} that falls below the slope part of the contour line of $FS = 1.0$.

For failure region 1, the slip surface is essentially circular and contained in the upper layer as shown in Fig. 4. For failure region 2, a deep failure mechanism is caused by the low strength of the lower layer and the slip surface is non-circular as shown in Fig. 5. For failure region 3, two failure mechanism can coexist at the same time as shown in Fig. 6. It should be mentioned that the ordinary method of slices and simplified Bishop method use circular slip surface and are not applicable for failure region 2. Failure region 2 was ignored when circular slip surface was used (e.g., Fig .7 in Ching et al. 2009).

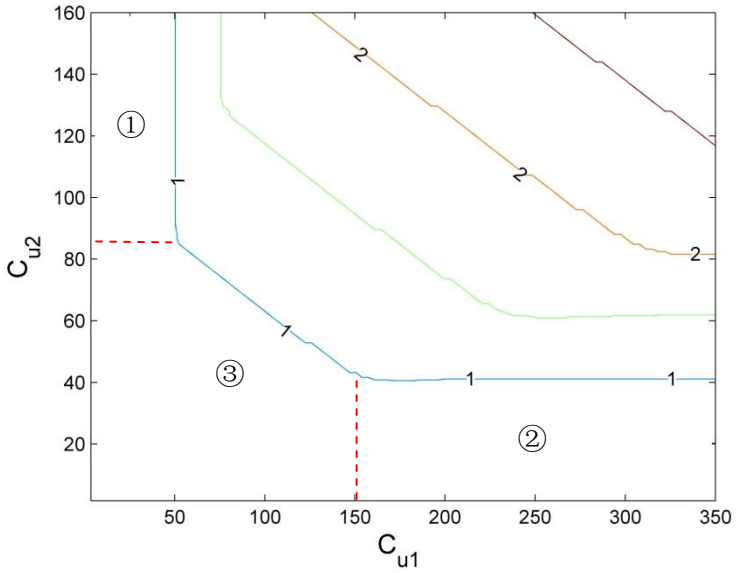

Fig. 3 Contour of factor of safety

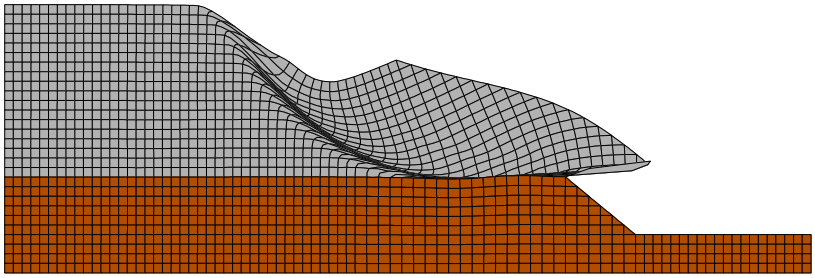
Fig. 4 Deformed mesh at failure when $c_{u1} = 45.0$ kPa , $c_{u2} = 160.0$kPa , $FS = 0.89$

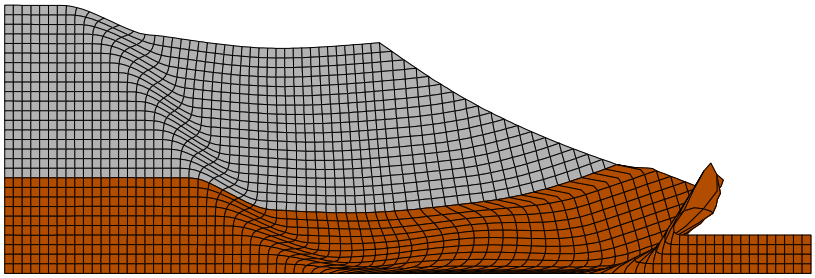
Fig. 5 Deformed mesh at failure when $c_{u1} = 120.0$ kPa , $c_{u2} = 30.0$kPa , $FS = 0.76$

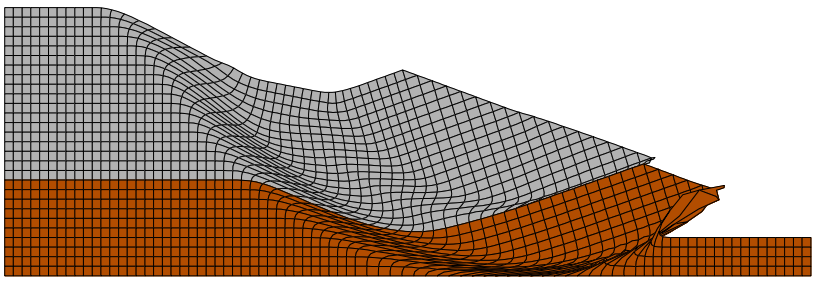
Fig. 6 Deformed mesh at failure when $c_{u1} = 46.0$ kPa , $c_{u2} = 75.0$kPa , $FS = 0.89$

PROBABILISTIC ANALYSIS

The undrained shear strengths c_{u1} and c_{u2} are assumed to be random variables characterized statistically by lognormal distributions. The mean values are $\mu_{c_{u1}} = 120\text{kPa}$ and $\mu_{c_{u2}} = 160\text{kPa}$ respectively. The coefficient of variation for both c_{u1} and c_{u2} are $V_{c_{u1}} = V_{c_{u2}} = 0.3$. In this study, 100,000 simulations were performed for each case. Each layer is independent and given a value at random from their respective distributions. The influence of the number of simulations on pf is shown in Fig. 7 and it can be seen from Fig. 7 that 40,000 simulations are sufficient to obtain reasonably repeatable results.

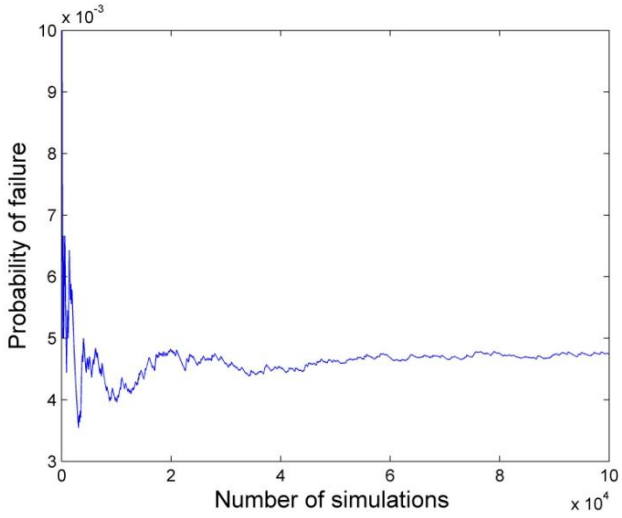

Fig. 7 Probability of failure verse number of simulations

The p_f estimated by 100,000 simulations is p_f =0.0047. The coefficient of variation of p_f is approximately (e.g., Fenton and Griffiths 2008),

$$V_{p_f} \simeq \sqrt{\frac{(1-p_f)}{n_{sim} p_f}} = 0.047 \tag{1}$$

where n_{sim} is the number of simulations.

The results are compared with Ching et al. (2009) and Low et al. (2011) in Table 1.

Table 1 Comparison of p_f

	Ching et al. (2009)	Low et al. (2011)		This paper
		Lower bound	Upper bound	
p_f	0.0044	0.0042	0.0044	0.0047
V_{p_f}	0.15			0.046
n	10,000			100,000

Since LEM ignored failure region 2 (e.g., Fig .7 in Ching et al. 2009), the p_f estimated in this study is higher than that obtained by Ching et al. (2009) and Low et al. (2011). The difference can be estimated by integration over failure region 2 as

$$\begin{aligned} p_{f\ region3} &= p\left[c_{u1} \geq 150\right] \times p\left[c_{u2} \leq 40\right] \\ &= \Phi\left(\frac{\mu_{\ln c_{u1}} - \ln 150}{\sigma_{\ln c_{u1}}}\right)\Phi\left(\frac{\ln 40 - \mu_{\ln c_{u2}}}{\sigma_{\ln c_{u2}}}\right) \\ &= 0.00056 \end{aligned} \tag{2}$$

where $\sigma_{\ln c_{u1}}$, $\mu_{\ln c_{u1}}$, $\sigma_{\ln c_{u2}}$ and $\mu_{\ln c_{u2}}$ are obtained by

$$\begin{aligned} \sigma_{\ln c_{u1}} &= \sqrt{\ln\left\{1+V_{c_{u1}}^2\right\}} \\ \mu_{\ln c_{u1}} &= \ln \mu_{c_{u1}} - \frac{1}{2}\sigma_{\ln c_{u1}}^2 \end{aligned} \tag{3}$$

The histogram of FS obtained in this study (using at least 50,000 simulations) led to the two distinct distributions shown in Fig. 8. The link between the distributions and the nature of the failure mechanisms is currently under further investigation.

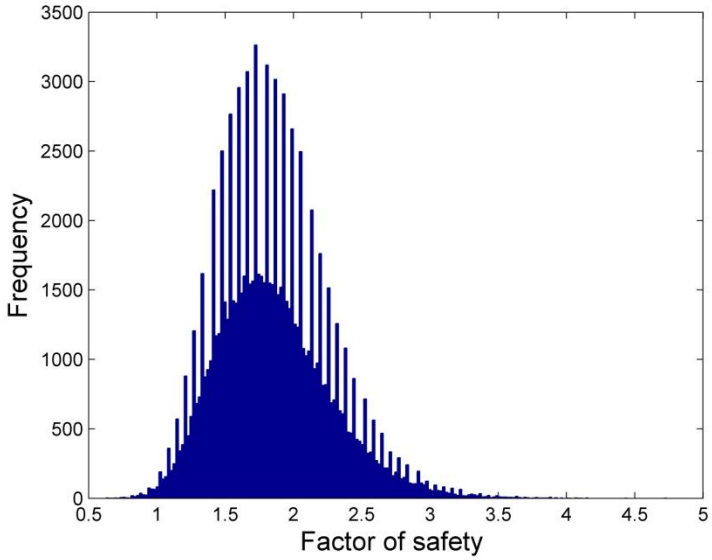

Fig. 8 Histogram of factor of safety from 100,000 simulations

INFLUENCE OF SPATIAL VARIABILITY ON p_f

RFEM (Griffiths and Fenton 2000, 2004 and Fenton and Griffiths 2008) has used to investigate the influence of spatial variability on p_f. The RFEM uses elastoplasticity in a finite-element model combined with random field theory in a Monte-Carlo framework. The input parameters relating to the mean, standard deviation and spatial correlation length are assumed to be defined at the "point" level. Full account is taken of local averaging and variance reduction (Fenton and Vanmarcke 1990) over each element. Since the actual undrained shear strength field is lognormally distributed, its logarithm yields an "underlying" normally distributed (or Gaussian) field. The spatial correlation length is measured with respect to this underlying field. The spatial correlation length (e.g. $\theta_{\ln c_{u1}}$) describes the distance over which the spatially random values will tend to be significantly correlated in the underlying Gaussian field. Thus, a large value of $\theta_{\ln c_{u1}}$ will imply a smoothly varying field, while a small value will imply a ragged field. In this work, an exponentially decaying (Markovian) correlation function is used of the form, for example:

$$\rho(\tau) = e^{-\frac{2\tau}{\theta_{\ln c_{u1}}}} \tag{4}$$

where $\rho(\tau)$ is the correlation coefficient between properties assigned to two points in the random field separated by an absolute distance τ.

In the current study, the spatial correlation length has been non-dimensionalized by dividing it by the height of the embankment H and will be expressed in the form, for example:

$$\Theta_{c_{u1}} = \theta_{\ln c_{u1}} / H \tag{5}$$

In order to study the p_f of layered slopes, the RFEM was further developed to have the ability to simulate multiple independent random fields. Fig. 9 and 10 show two typical simulations at failure. The figure depicts the variation of c_{u1} and c_{u2}, and have been scaled in such a way that dark and light regions depict "strong" and "weak" soil respectively. When two failure mechanisms coexist at the same time, Fig. 9 suggests that using rigid slices in LEM is inappropriate. Furthermore, it can be seen from Fig. 10 that the failure mechanism is non-circular. Both these examples suggest that the use of Limit Equilibrium Methods with circular slip surfaces is inappropriate.

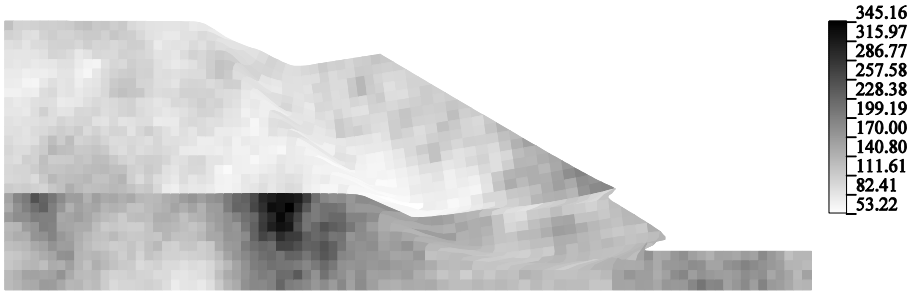

Fig. 9 Typical simulation when $\Theta_{c_{u1}} = \Theta_{c_{u2}} = 1.0$, $FS = 1.58$

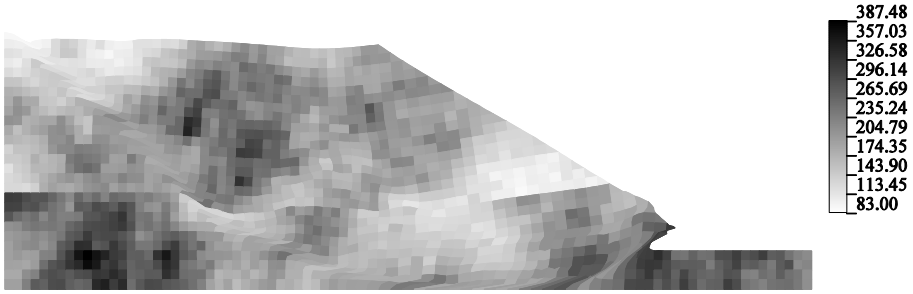

Fig. 10 Typical simulation when $\Theta_{c_{u1}} = \Theta_{c_{u2}} = 1.0$, $FS = 2.68$

The influence of spatial variability on p_f was studied by varying $\Theta_{c_{u1}} = \Theta_{c_{u2}}$ in the range {0.5, 1.0, 2.0, 4.0, 8.0, 16.0, 32.0, 64.0, 128.0, 256.0, 512.0}. For cases when $\Theta_{c_{u1}} = \Theta_{c_{u2}} = \{0.5,\ 1.0,\ 2.0\}$, one million simulations were conducted. For other cases, One hundred thousand simulations were conducted. Table 2 shows the influence of spatial variability on p_f. Also shown in Table 2 is the coefficient of variation of p_f. It should be mentioned that for case when $\Theta_{c_{u1}} = \Theta_{c_{u2}} = 0.5$, there was no failure from one million simulations.

It can be seen from Table 2 that decreasing spatial variability will decrease p_f. It is interesting to note that when $\Theta_{c_{u1}} = \Theta_{c_{u2}} \geq 32.0$, the influence of spatial variability on p_f is negligible.

Table 2. Influence of spatial variability on p_f

$\Theta_{c_{u1}} = \Theta_{c_{u2}}$	$\hat{p}_f$	n_{sim}	$V_{\hat{p}_f}$
0.5	<1E-6	1000000	
1	4.70E-05	1000000	0.145862
2	5.22E-04	1000000	0.043757
4	0.0016	100000	0.078994
8	0.0027	100000	0.060776
16	0.0038	100000	0.051201
32	0.0046	100000	0.046518
64	0.0046	100000	0.046518
128	0.0047	100000	0.046018
256	0.0046	100000	0.046518
512	0.0047	100000	0.046018

CONCLUSIONS

A benchmark two layer slope for system reliability analysis is presented. Deterministic analysis showed that there are three failure regions associated with different combinations of shear strength of the two layers. Probabilistic analysis showed that p_f obtained by FEM is consistently higher than that obtained by LEM. The histogram of factor of safety from 100,000 simulations showed clearly two failure modes. Probability of failure decreases with increasing spatial correlation length.

ACKNOWLEDGEMENTS

The authors wish to acknowledge the support of (i) The Australian Research Council Centre of Excellence for Geotechnical Science and Engineering (ii) NSF Grant CMMI-0970122 on "GOALI: Probabilistic Geomechanical Analysis in the Exploitation of Unconventional Resources."

REFERENCES

Ching, J., Phoon, K.K. and Hu, Y.G., (2009). "Efficient Evaluation of Reliability for Slopes with Circular Slip Surfaces Using importance Sampling." *Journal of Geotechnical and Geoenvironmental Engineering*, Vol. 135(6):768-777

Chowdhury, R. N. and Xu, D. W., (1995). "Geotechnical system reliability of slopes." *Reliability Engineering and System Safety*, 47:141-151

Cornell, C. A., (1967). “Bounds on the Reliability of Structural Systems.” *J. Struct. Div., ASCE,* 93:171-200.

Fenton, G. A., and Griffiths, D. V., (2008). *“Risk Assessment in Geotechnical Engineering.”* John Wiley & Sons, New York.

Fenton, G. A., and Vanmarcke, E. H., (1990). Simulation of random fields via local average subdivision. *J Eng Mech, ASCE,* 116(8):1733–1749

Griffiths, D. V., and Fenton, G. A. (2000). " Influence of soil strength spatial variability on the stability of an undrained clay slope by finite elements." *Slope stability 2000,* Geotechnical Special Publications No. 101, ASCE, 184‑193

Griffiths, D. V., and Fenton, G. A. (2004). “Probabilistic slope stability analysis by finite elements.” *ASCE Journal of Geotechnical and Geoenvironmental Engineering,* 130(5): 507-518.

Griffiths, D. V. and Lane, P. A. (1999). “Slope stability analysis by finite elements.” *Géotechnique,* 49(3):387–403.

Huang, J., Griffiths, D.V., and Fenton, G.A., (2010). "System reliability of slopes by RFEM." *Soils and Foundations*, Vol.50(3):343-353

Low, B.K., Zhang, J. and Tang, W.H., " (2011). "Efficient system reliability analysis illustrated for a retaining wall and a soil slope." *Computers and Geotechnics,*Vol.38:196-204

Oka, Y. and Wu, T. H., (1990), “System Reliability of Slope Stability.” *J. Geotechnical Engng, ASCE,* 116:1185-1189.